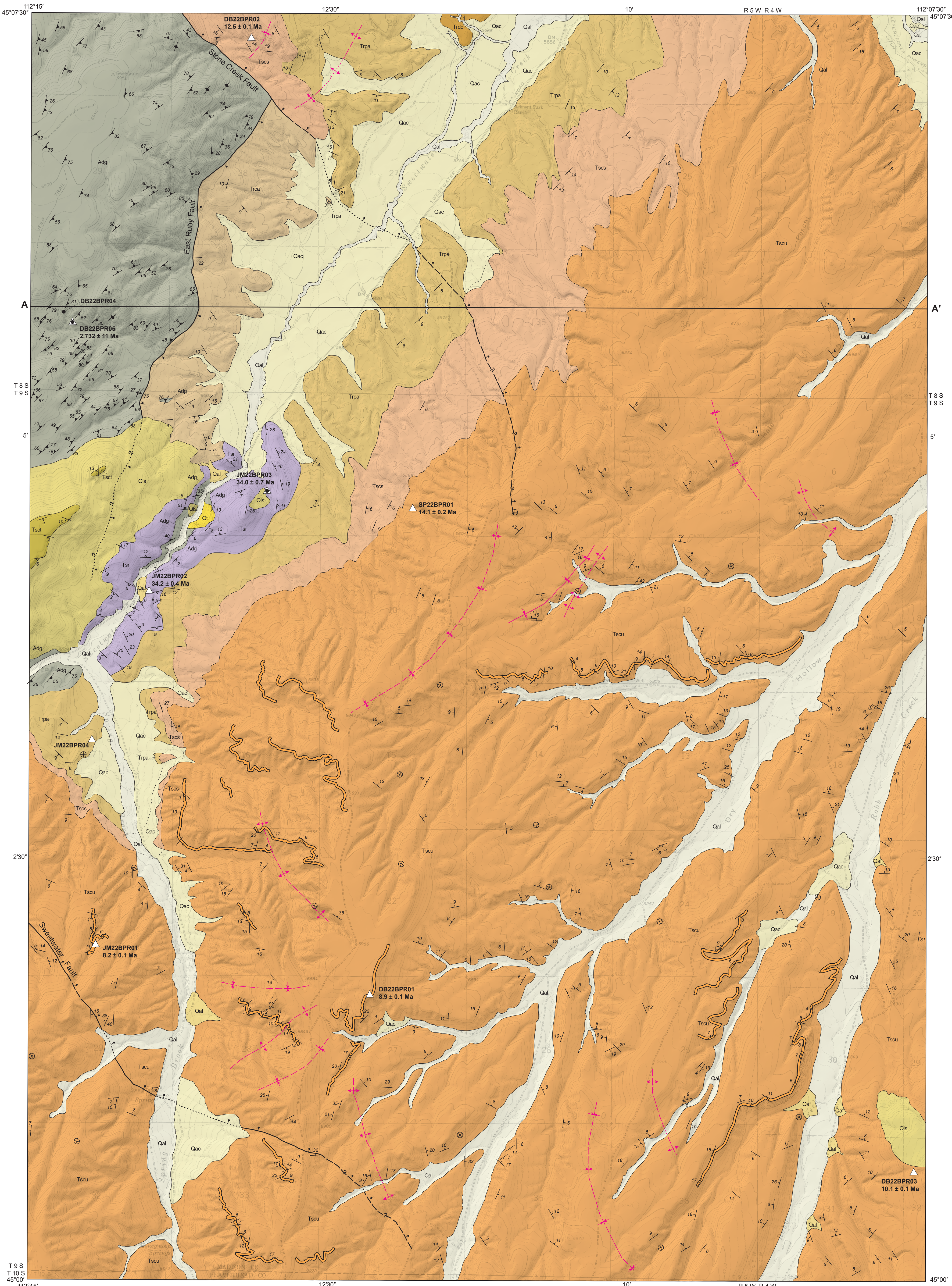

Base map produced by the United States Geological Survey
Belmont Park Ranch 1:24,000-scale quadrangle map
Control by: USGS and USC&GC
Compiled from aerial photographs taken 1961
Field checked: 1963
Projection: Polyconic
Vertical Datum: National Geodetic Vertical Datum of 1929
Horizontal Datum: 1927 North American Datum

Shaded relief created from 10-meter digital elevation model from U.S. Geological Survey National Elevation Dataset.

SCALE 1:24,000

CONTOUR INTERVAL 40 FEET
NATIONAL GEODETIC VERTICAL DATUM OF 1929

UTM GRID AND 2019 MAGNETIC NORTH DECLINATION AT CENTER OF SHEET

Maps may be obtained from:
Publications Office
Montana Bureau of Mines and Geology
1300 West Park Street
Butte, Montana 59701-8997
Phone: (406) 496-4174
https://mbmg.mtech.edu

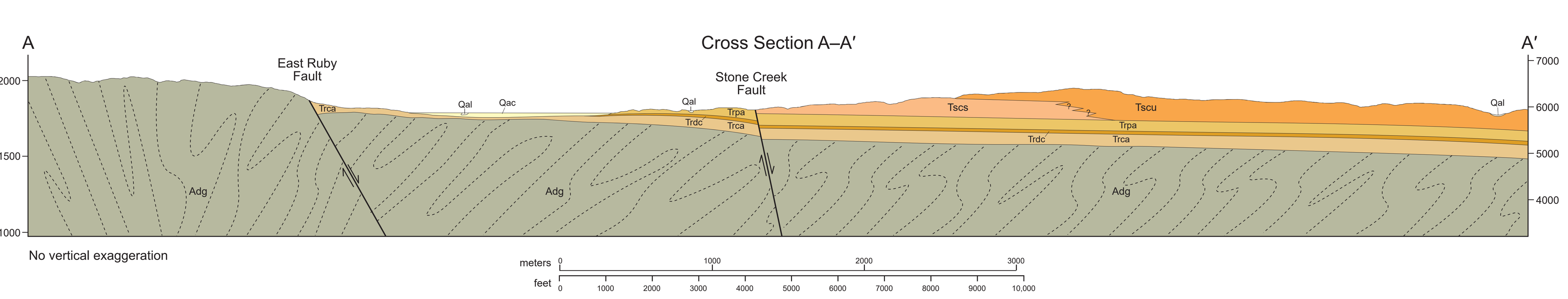

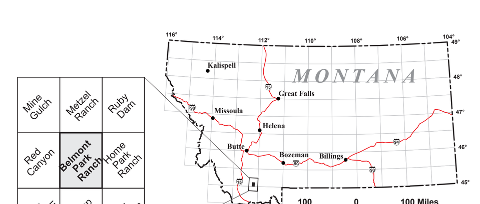

Research supported by the U.S. Geological Survey, National Cooperative Geologic Mapping Program, under USGS award G22AC00376.
GIS production: Daniel Brennan, Patricia Ekberg, and Yiwen Li, MBMG. Map layout: Susan Smith, MBMG. Editing: Susan Barth, MBMG.

CORRELATION CHART

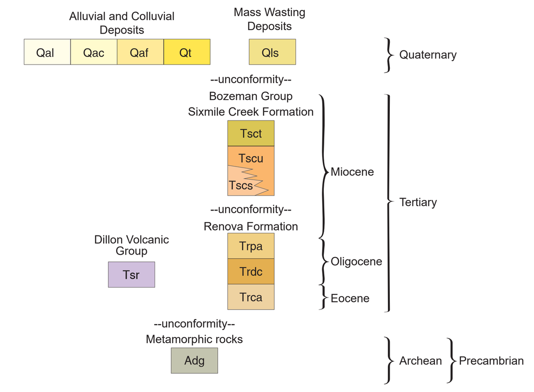

MAP SYMBOLS

Contacts, Faults, and Structure lines

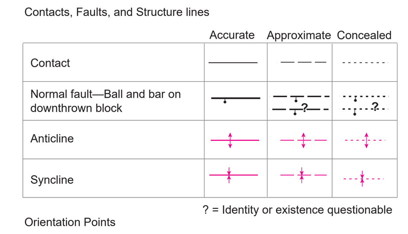

Orientation Points

- Horizontal bedding
- Inclined bedding—Showing strike and dip
- Inclined flow banding, lamination, layering, or foliation in igneous rock—Showing strike and dip
- Inclined metamorphic or tectonic foliation—Showing strike and dip
- Vertical metamorphic or tectonic foliation—Showing strike
- Sample: Bulk rock geochemistry (Table 1)
- Sample: U-Pb geochronology (Table 2)

PHYSIOGRAPHIC AND TECTONIC SETTING

The Belmont Park Ranch 7.5′ quadrangle is located in Madison County, Montana, approximately 40 km (24.9 mi) southeast of Dillon and 25 km (15.5 mi) south of Alder (fig. 1). The quadrangle comprises much of the southwestern part of the upper Ruby River Valley, about 8 km (5 mi) south of the Ruby River Reservoir. The upper Ruby River Valley is bounded by predominately northeast–southwest-trending mountain ranges, the Ruby Range to the northwest and the Snowcrest, Greenhorn, and Gravelly Ranges to the southeast (fig. 1). The modern topography in the region generally reflects Basin and Range extension and/or collapse of the thickened Cordillera during the Eocene to present (Constenius, 1996). Exposure of bedrock geology in the Belmont Park Ranch quadrangle is generally fair, and includes Archean to Paleoproterozoic metamorphic basement rocks and noteworthy exposures of Tertiary (Paleogene and Neogene) rocks of the Dillon Volcanic Group and the Bozeman Group.

The northwest-flowing Ruby River traverses the very northeast corner of the Belmont Park Ranch quadrangle. The Ruby River's tributaries, including the perennial Sweetwater and Robb Creeks, and their respective named tributaries, the perennial Spring Brook and ephemeral Dry Hollow Creek, drain the majority of the map area. The quadrangle is characterized by moderate relief with elevations ranging from 1,700 to 2,128 m (5,580 to 6,980 ft) above sea level, and is composed of Dry Gneissic–Schistose–Volcanic Hills and Dry Intermontane Sagebrush Valleys ecoregions. The natural vegetation of this semiarid region is mostly sagebrush steppe with an average annual precipitation from 30 to 56 cm (12 to 21 in). Grazing, wildlife habitat, and irrigation-supported farming in the bottomlands are common land uses (Woods and others, 2002).

GEOLOGIC SUMMARY

The oldest rock units are exposed within the Ruby Range in the northwestern part of the map area and are composed of primarily gneiss and intercalated amphibolite bodies, which both generally display a regional northeast–southwest–trending foliation, and are collectively mapped as the Archean Dillon Gneiss (Adg). The Dillon Gneiss formed by ca. 2.9–2.6 Ma. Elsewhere within the Ruby Range temporally distinct ca. 2.5–2.4 Ga and ca. 1.8 Ga tectonothermal events are also reported (Harms and Baldwin, 2020 and references within). The Dillon Gneiss (Adg) is in fault contact with, or unconformably overlain by, late Eocene rocks of the Dillon Volcanic Group, poorly consolidated Tertiary strata of the Bozeman Group, or younger unconsolidated Quaternary deposits. Within the map area, ca. 34 Ma rocks of the Dillon Volcanic group (Tsr) are primarily felsic in composition and exposed along Sweetwater Creek. The remainder of the quadrangle contains noteworthy exposures of the Tertiary Bozeman Group, including the Renova (Trca, Trdc, Trpa) and overlying Sixmile Creek (Tscs, Tscu, Tsct) Formations. Here, the Renova Formation is generally fine-grained, while the Sixmile Creek Formation contains coarser conglomerates/breccias along with interbedded tephra deposits (dated at ca. 14.1 to 8.2 Ma), and localized volcanic flows such as the ca. 6 Ma Timber Hill Basalt (Tsct; Fritz and others, 2007). The Timber Hill Basalt forms a prominent mesa along the western portion of the map area where it overlies more recessive Sixmile Creek sedimentary members. Mesoproterozoic to Cretaceous rocks are absent within the map area, suggesting their complete exhumation or non-deposition prior to deposition of the Renova Formation in the late Eocene.

Recognized faults are limited to two northwest-trending faults, the Sweetwater and Stone Creek faults, and one northeast-trending fault, the East Ruby fault. Although no faults were found to cut Quaternary units within the map area, to the northwest the Stone Creek fault is shown to cut Quaternary deposits (Stotter, 2019), and the Sweetwater Fault is also inferred to have been active in the Quaternary (Mosolf and Sears, 2023). Within the map area, the northeast-trending East Ruby fault is truncated by the northwest-trending Stone Creek fault, suggesting the northwest-trending fault set is the younger feature. Prior workers (e.g., Fritz and Sears, 1993) have related the northwest-trending fault in the region to passage of the Yellowstone hotspot and associated crustal doming. Quaternary alluvium (Qal), alluvium and colluvium (Qac), and alluvial fan deposits (Qaf) are common along the Sweetwater Creek, Rob Creek, Dry Hollow, and Spring Brook drainages. Where undercut and over-steeped slopes have formed along Sweetwater Creek, Quaternary Landslide (Qls) and Talus (Qt) deposits are also present.

PREVIOUS MAPPING

The Belmont Park 7.5′ quadrangle is included in a small-scale (1:250,000-scale) geologic map by Ruppel and others (1993) and parts of the quadrangle are included in larger-scale (1:24,000-scale) thesis mapping of Monroe (1976), Ripley (1987), and Garson (1992).

METHODS

Field Mapping

Geologic mapping in the Belmont Park Ranch 7.5′ quadrangle was conducted over the 2022 field season as part of the U.S. Geological Survey (USGS) STATEMAP program, a component of the National Cooperative Geologic Mapping Program (NCGMP). A 1:24,000-scale topographic base was utilized for field mapping, and geologic contacts were refined using the orthoimagery dataset produced by the National Agricultural Imagery Program (NAIP; 2018–2020). Structure and observational data were located using a handheld GPS device; structure data were measured with a traditional hand transit or mobile device. Field sheets were scanned and georeferenced in GIS software. The geologic data were subsequently digitized to the Geologic Map Schema (GeMS) geodatabase of the NCGMP.

Geochemistry and U-Pb Geochronology

Rock samples collected for whole-rock geochemistry and U-Pb geochronology were processed at the MBMG mineral separation laboratory. A ~100–200 g split of the crushed material was prepared for bulk-rock geochemical analysis and subsequently analyzed by X-ray fluorescence (XRF) and inductively coupled plasma mass spectrometry (ICP-MS) at the Peter Hooper GeoAnalytical Lab, Washington State University. Zircon was isolated from select specimens by standard density and magnetic separation techniques at the MBMG mineral separation laboratory. Zircon separates were then analyzed by laser ablation inductively coupled plasma mass spectrometry (LA-ICP-MS) at the University of California, Santa Barbara.

Whole-rock chemical data acquired from this map area (Mosolf and others, 2023a) are provided in table 1. Zircon U-Pb geochronology results (Mosolf and others, 2023b) are provided in figure 2 and summarized in table 2.

DESCRIPTION OF MAP UNITS

Unconsolidated and Geomorphic Units

Qal **Alluvium (Quaternary: Holocene)**—Unconsolidated, well-rounded, moderate to well sorted cobbles, gravel, sand, and silt deposited in active stream channels and floodplains. Thickness generally less than 6 m (20 ft).

Qac **Alluvium and Colluvium (Quaternary: Holocene)**—Dominantly sand, silt, clay, and subordinate gravel and cobbles locally, deposited on relatively gentle slopes primarily by sheetwash and gravity processes. Thickness generally less than 10 m (33 ft).

Qaf **Alluvial Fan Deposits (Quaternary: Holocene)**—Unconsolidated, moderately to poorly sorted, locally derived deposits composed of silt and sand with subangular to subrounded boulder-size clasts. Deposits formed as coalescent alluvial fan channels to debris flow fans along the front of steep hillslopes. Thickness as much as 15 m (50 ft).

Qt **Talus Deposits (Quaternary: Holocene)**—Unconsolidated, locally derived deposits of angular clasts on and below steep slopes. Variable thickness, generally less than 10 m (33 ft).

Qls **Landslide Deposits (Quaternary)**—Unconsolidated, unsorted, and unstratified mixtures of proximally derived angular material, forming characteristic irregular hummocky topography due to downslope movement related to mass wasting processes. Some deposits may be currently or recently active as evidenced by limited denudation of head scarps. The most significant landslides are associated with over steepening and undercutting of slopes where resistant volcanic rocks of the Timber Hill Basalt (Tsct) of the Sixmile Creek Formation overlie more recessive Sixmile Creek Formation members. Variable thicknesses as much as 15 m (50 ft).

Bozeman Group

Here, we utilize the Bozeman Group nomenclature of Kuenzi and Fields (1971). The Bozeman Group consists of two formations, the predominantly fine-grained Eocene–lower Miocene, Renova Formation, and the unconformably overlying upper Miocene–Pliocene, predominately coarse-grained Sixmile Creek Formation. Petkewich (1972) applied the Kuenzi and Fields (1971) Renova Formation nomenclature to rocks near Dillon, and recognized four mappable members: (a) Climbing Arrow, (b) Dunbar Creek, (c) Williams Creek basalt, and (d) Passamari. Monroe (1976) recognized three (the Climbing Arrow, Dunbar Creek, and Passamari) of these four members within the Ruby Valley.

Within the Ruby Valley, Monroe (1976) also subdivided the Sixmile Creek Formation into three informal, lithologically defined members: the metamorphic fanglomerate, feldspathic sandstone, and quartzite pebble conglomerate members. Fritz and Sears (1993) revised this Sixmile Creek nomenclature into three spatially and temporally interleaved lithologic units consisting of the Sweetwater Creek, Anderson Ranch, and Big Hole River members, and one volcanic flow—the Timber Hill Basalt. Within the Belmont Park Ranch quadrangle, proximally derived predominately subangular conglomerates, interpreted as fanglomerate deposits of the Sweetwater member (Tscs), occupy a consistent basin margin location and can be delineated at 1:24,000-scale. Anderson Ranch tephra beds are interbedded with round quartzite cobble conglomerates of Big Hole River member and do not always occur in a consistent stratigraphic order. The Sixmile Creek Formation is best exposed along south-facing slopes in the eastern part of the quadrangle. Anderson Ranch tephra and Big Hole River round cobble conglomerate lithologies commonly crop out and are interbedded at the meter scale. Due to the interbedded relationship, we refer to the tephra intervals as Anderson Ranch beds, not members.

Sixmile Creek Formation (Miocene)— A poorly consolidated sequence of interbedded conglomerate and coarse sandstone beds (Monroe, 1976), with lesser intervals of mudstone and tephra. The Big Hole River member and Anderson Ranch beds were mapped as an undivided unit (Tscu). Anderson Ranch beds extensive enough to be mapped at 1:24,000 scale are shown with lines. The Sweetwater Creek member (Tscs) and Timber Hill Basalt (Tsct) were mapped separately. Previously published radiometric age dates for the Sixmile Creek Formation span 16–3.7 Ma, consistent with fossil ages (Monroe, 1976; Fritz and Sears, 1993). U-Pb zircon dates collected in this study have calculated ages of 14.1 to 8.2 Ma (fig. 2A), and contain older zircon grains that range from 2,900 to 80 Ma (fig. 2B). Estimated total thickness of all members combined is at least 460 m (1,510 ft).

Tsct **Timber Hill Basalt, informal (late Miocene)**—Reddish-gray to black vesicular basalt flow. Contains phenocrysts of plagioclase, altered pyroxene, and trace amounts of hornblende and magnetite in a dark groundmass (Garson, 1992). Forms a resistant ridge that can be traced approximately 60 km (37 mi) to the southwest (Fritz and Sears, 1993). Exposures within this map area represent the units, most northern known extent. The Timber Hill Basalt overlies rounded, likely fluvial, gravels and conglomerates of the Sixmile Creek Formation, suggesting the basalt flowed down a paleochannel. Reported K-Ar whole-rock ages span from 6.3 ± 0.2 Ma to 5.9 ± 0.2 Ma (Fritz and others, 2007). Unit is approximately 12 m (40 ft) thick.

Tscu **Sixmile Creek Formation, undivided (late to middle Miocene)**—Predominately coarse-grained, clast-supported conglomerate of the Big Hole River member interstratified with Anderson Ranch tephra beds. Bioturbation, Hemphillian-age vertebrate fossils, and soft sediment deformation are typical throughout the unit. Paleosol horizons are also present. Intraformational low-angle unconformities, clastic dikes, and syndepositional fault and/or soft sediment compaction features are commonly observable, indicating tectonically active deposition (fig. 3). Gentle folds within this unit are likely associated with intrabasinal faulting, and differential compaction of beds during burial. Mapped relationships suggest this unit may be as thick as 300 m (984 ft).

Big Hole River member, informal—Black, green, red, pink, and white, well-rounded, polymictic cobble to pebble conglomerate, with lesser coarse-grained feldspathic and lithic sandstone intervals. Clasts are predominantly quartzite and argillite, with lesser chert and volcanics. Locally, volcanic clasts are moderately abundant, generally in the lower stratigraphic horizons. However, even where most abundant, volcanic clasts are still a subordinate clast component (<20 percent), generally rounded, and not accompanied with gneiss or schist basement clasts, distinguishing the Big Hole River member from the Sweetwater member. Clastic grain sizes range primarily from silt to cobbles (<25 cm, 10 in); however, rare boulders (<40 cm, 16 inches) can be found. Channelization is typical, with abundant large-scale planar and festoon cross-bedding. Load structures, including flame structures and clastic dikes, are locally present. Many beds grade laterally or vertically from sandstone to conglomerate, with gravel lenses in sandstone beds typical. Conglomeratic deposits are typically well stratified, although some massive intervals are present. Coarser, predominately cobble conglomerate intervals are almost exclusively clast-supported, but finer intervals and gravel lenses are often supported in a sandy matrix. Meter-scale intervals of darker gray/brown color, extensive root casts, and more resistant outcrop patterns are also present and interpreted as paleosol horizons. Locally, offset of beds below a non-offset paleosol horizon can be found and are interpreted to record syndepositional faulting (fig. 3). Conglomerate horizons within individual outcrops are as thick as 15 m (50 ft); total map unit thickness is approximately 110 m (360 ft).

Anderson Ranch beds, informal—White to light gray, tabular to lenticular bedded, trough cross-bedded, fluvially reworked and air-fall tephra deposits. Tephra is a mix of ash and pumice, often interbedded with silicic sand and gravel, and intrabasinal rip-up clasts. Rip-up clasts range from rounded pebbles to large angular fragments of finer-grained tephra and pumice (Thomas and Sears, 2020). Locally, pumice pebble conglomerate beds are present. Monroe (1976) reports that the absence of bentonitic clay distinguishes this unit from tephra-rich members of the underlying Renova Formation. U-Pb zircon dates of tephra interbedded with the Big Hole River member collected in this study have calculated ages of 14.1 to 8.2 Ma (fig. 2A, table 2). We note that the North American Stratigraphic Code (NACSN, 2021) specifies that stratigraphic members may contain beds or flows, but may never contain other members. Thus, we informally refer to these tephra intervals as beds, while prior workers (Fritz and Sears, 1993; Thomas and Sears, 2020) have referred to them as spatially and temporally interleaved informal members. This map unit delineates well-exposed and continuous tephra beds. Up to 30 m (100 ft) thick.

Tscs **Sweetwater member, informal (Miocene)**—Yellowish gray, light gray, and reddish gray, predominantly conglomerate with distinctly subangular to angular boulders as much as 2 m (6 ft) in diameter. Clast lithologies include basement rocks (gneiss and schist, often garnet-bearing) with lesser vesicular volcanic, pegmatite, quartzite, and coarse-grained, feldspathic, and lithic-rich sandstone. Localized beds of siltstone, limestone, and tuff are present in subordinate amounts. Conglomerate-filled channels are locally common. Clast sorting is generally poor. At outcrop scale, bedding is often indistinct or crudely stratified. A tephra interval sampled from this unit gave a zircon U-Pb weighted mean age of 12.5 ± 0.1 Ma, indicating that deposition of the Sweetwater member was contemporaneous with the Big Hole River member in this area. As thick as 150 m (492 ft) thick and thins to the southwest within the map area.

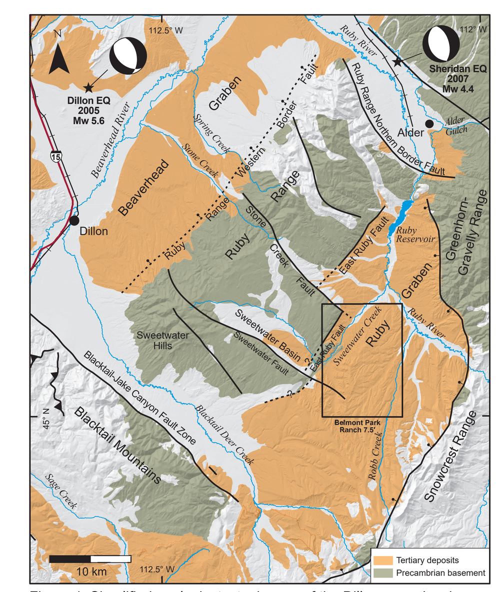

Figure 1. Simplified geologic–tectonic map of the Dillon area showing the major structures and geologic units discussed in the text. The rectangular box shows the location of the Belmont Park Ranch 7.5′ quadrangle. The geology is mostly derived from the geologic map of the Dillon 1° x 2° quadrangle (Ruppel and others, 1993) and overlain on a shaded digital elevation model (DEM).

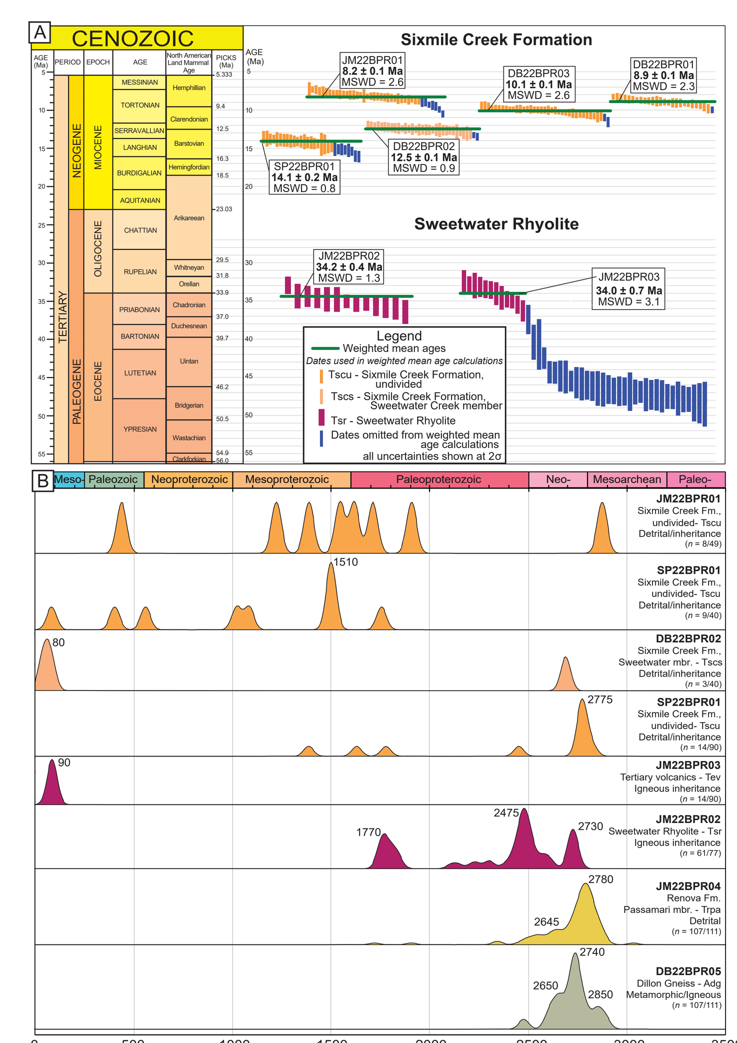

Figure 2. (A) Weighted mean ages of youngest Tertiary zircon populations from the Sixmile Creek and Eocene/Oligocene volcanic samples (all shown in ^{207}Pb corrected, $^{206}Pb/^{238}U$ dates), which are interpreted as volcanic and/or syndepositional ages. (B) Zircon kernel density estimate (KDE) plots (with 25 Myr bin and bandwidths) of U-Pb dates from the Sixmile Creek, Renova, and Eocene volcanic units, which are interpreted as inherited and/or detrital grains, and the Archean Dillon Gneiss, which are interpreted as metamorphic and/or igneous grains. KDE plots were calculated using the ^{207}Pb corrected, $^{206}Pb/^{238}U$ dates (<1000 Ma) and $^{207}Pb/^{206}Pb$ with no common Pb correction (>1000 Ma) ratios, and filtered to omit analyses greater than 20 percent discordant. Age-peaks consisting of more than a single analysis were labeled, rounded to the nearest 5 Ma. The number of analyses that meet this filter and are plotted out of the total number of analyses is indicated (n = number of analyses plotted/total number of analyses).

Complete geochronology data available from Mosolf and others (2023b).

Renova Formation (Eocene to Oligocene)—Composed primarily of fine-grained rocks consisting of shale, mudstone, limestone, and medium- or fine-grained sandstone beds that largely reflect fluvial and lacustrine deposition (Kuenzi and Fields, 1971; Monroe, 1976; Vuke, 2020), making it distinct from the younger, mostly coarser-grained Sixmile Creek Formation. Three members of the Renova Formation, described below, are recognized within the map area—the basal Climbing Arrow, and overlying Dunbar Creek and Passamari Members. Estimated total thickness of the three members is at least 175 m (575 ft).

Trpa **Passamari Member (late Oligocene to early Miocene)**—Consists of a lower and upper interval. The upper interval is composed of light tan, fine-grained shales that vary from thinly bedded and fissile with small amounts of volcanic ash to silty, blocky-weathering, and lacking volcanic ash. An upper interval is very light buff and light gray, calcareous, thinly bedded shales with fine sand and clay horizons. The Passamari Member commonly forms low rounded hills with generally poor outcrops limited to recent erosional gullies. This unit is interpreted as lacustrine with local conglomerates reflecting deltaic deposition. Contact with the underlying Dunbar Creek Member is not exposed in the upper Ruby River Valley (Monroe, 1976). Upper contact is generally a low (<10 degree) angular unconformity with the overlying basal Sweetwater member of the Sixmile Creek Formation. At least 70 m (230 ft) thick.

Trdc **Dunbar Creek Member (Oligocene)**—Greenish-gray to light brown, primarily siltstone sequence with mudstone, lesser sandstone, and rare tuffaceous interbeds (Monroe, 1976). Commonly forms a distinct "popcorn" weathering surface and gradationally overlies the Climbing Arrow Member. Outcrops are rare with limited exposure along low-relief hills in sections 22 and 23 (T. 8 S., R. 5 W.). Approximately 40 mi (64 km) north of the map area, in the Jefferson Basin, the Dunbar Creek Member is approximately 180 to 300 m thick (~600 to 1,000 ft; Kuenzi and Fields, 1971; Monroe 1976) but in this map area, only ~24 m (~80 ft) is exposed.

Trca **Climbing Arrow Member (Eocene)**—Poorly exposed light gray to pale orange and brown mudstone with lesser amounts of quartz–biotite sandstone. In the upper Ruby River Valley, the Climbing Arrow Member can be differentiated from the overlying Dunbar Creek Member by its rare conglomerate and limestone interbeds, complete lack of tuffaceous horizons, and significantly less siltstone. A minimum thickness of at least 80 m (~260 ft) is exposed.

Tertiary Volcanics

Tsr **Sweetwater Rhyolite (late Eocene to early Oligocene)**—Pink, maroon, tan, and gray, interbedded rhyolite (table 1) and volcaniclastic tuff. Rhyolites are mostly aphanitic with some quartz phenocrysts. Volcanic units are interbedded with locally cross-bedded, lithic/feldspathic and tuffaceous sandstones. Sandstones are coarse, locally pebble conglomerates containing subangular, polymictic lithics. U-Pb geochronology results yield a ca. 34 Ma depositional age for this unit (fig. 2A, table 2), suggesting volcanism was contemporaneous with the Virginia City Volcanic Group (Mosolf, 2021) approximately 25 km (16 mi) to the northeast. As thick as 180 m (600 ft) thick.

Precambrian Metamorphic and Intrusive Rocks

The only recognized Precambrian unit in the map area is the Dillon Gneiss, the name used by Heinrich (1960) and Garihan (1979) for the massive-to-foliated quartzofeldspathic/granitic gneiss with abundant intercalations of amphibolite within the Ruby Range, and equivalent to the Quartzofeldspathic Gneiss unit of James (1990). The Dillon Gneiss has been considered a western exposure of ca. 2.8 Ga Neoarchean rocks of the Wyoming Province, and likely experienced several younger Precambrian tectonothermal pulses at ~2,500–2,400 Ma and 1,800–1,700 Ma (Harms and Baldwin, 2020; Mogk and others, 2020).

Adg **Dillon Gneiss (Archean)**—Light gray, tan to orange, strongly foliated, and commonly lineated quartzofeldspathic gneiss with intercalated quartz, aplite, and pegmatitic bodies. Mineralogy consists primarily of quartz, microcline, plagioclase, and minor biotite, locally garnetiferous. Crops out as resistant, thick, sheet-like masses usually along foliation planes. Hosts salt-and-pepper-colored, foliated amphibolite bodies parallel to foliation that are composed primarily of blocky amphibole with lesser, likely secondary quartz. Amphibolite bodies are as much as ~25 m (82 ft) thick. Originally named the "Dillon Granite Gneiss" (Heinrich, 1960) and subsequently referred to as the Quartzofeldspathic Gneiss (James, 1990). U-Pb zircon results for the Dillon Gneiss exhibit significant Pb-loss but concordant dates range from 2,890 to 2,480 Ma (fig. 2B).

STRUCTURAL GEOLOGY

Metamorphic basement rocks of the Dillon Gneiss are intensely deformed in the Ruby Range, and record several generations of deformation. Although there are multiple generations of folds, the main metamorphic foliation is mostly axial planar to isoclinal folding, with fold axes that generally trend northeast (~046°) with a plunge (~17°; fig. 5A). Regionally extensive Paleozoic and Mesozoic strata (e.g., Ruppel and others, 1993) are absent in the Belmont Park quadrangle, suggesting their complete exhumation and erosion, likely during Cordilleran contractional deformation, prior to Tertiary deposition of the Bozeman Group.

Tertiary Bozeman Group strata and older rocks within the map area are displaced by two generations of high-angle, northeast- and northwest-trending normal faults that accommodated Cenozoic extension. The southeast-dipping East Ruby fault (Ruppel and others, 1993) places Renova Formation rocks against the Dillon Gneiss. Based on Dillon Gneiss exposures in the hanging wall, throw along this mapped segment of the East Ruby fault is approximately 60 to 100 m (~200 to 330 ft). The trace of the fault to the southwest within Sixmile Creek and younger strata is not clearly mappable. Renova Formation sediments in proximity to the East Ruby fault are generally fine-grained, and coarse-grained Sixmile Creek strata (Sweetwater member) generally thins to the southwest. These relationships suggest that the most recent movement on the East Ruby fault was likely in the early Miocene after deposition of the Renova Formation, and movement post-middle Miocene deposition of the lower Sixmile Creek Formation (ca. 12.5 Ma) may have been limited.

The northern extent of the East Ruby fault is crosscut by the younger, generally northwest-trending Stone Creek fault. The Stone Creek fault downdrops upper Renova Formation (Passamari Member) and Sixmile Creek Formation (Sweetwater member) onto Dillon Gneiss and lower Renova Formation (Climbing Arrow Member). Within the map area, there is likely at least 180 m (~590 ft) of normal throw along the Stone Creek fault, but along its trace to the northwest, it may have significantly more throw and/or an earlier left-lateral offset (Garson, 1992). In the southwest part of the map, a similarly oriented northwest-trending fault, the Sweetwater fault, offsets Sixmile Creek Formation. To the northwest in the adjacent Red Canyon 7.5′ quadrangle (Mosolf and Sears, 2024), the Sweetwater Fault offsets the Timber Hill Basalt of the Sixmile Creek Formation, with approximately 200–250 m (720 ft) of normal throw. Consequently, movement on these northwest-trending faults appears to postdate movement on the northeast-trending East Ruby fault. Their orthogonal geometries suggest these northwest-trending faults may have originated as transfer faults to the northeast-trending East Ruby Fault, perhaps associated with long-lived crustal anisotropies (see Mosolf and Sears, 2024).

The Cenozoic units within the area generally show minimal folding (figs. 5B, 5C). Where folded into open synclines and anticlines, the folding may represent differential compaction of the strata in proximity to syn- and post-depositional faults, as evidenced by associated sedimentary compaction structures such as clastic dikes and flame structures.

ACKNOWLEDGMENTS

Connie Thomson, Stuart Parker, and Amanda Rossi assisted with mineral separations at the MBMG Mineral Separation Laboratory. Andrew Kylander-Clark supported LA-ICPMS analyses and data reduction at the University of California, Santa Barbara. Ashley and Arron Steiner directed bulk-rock geochemical analyses at the Washington State University Peter Hooper Geoanalytical Laboratory.

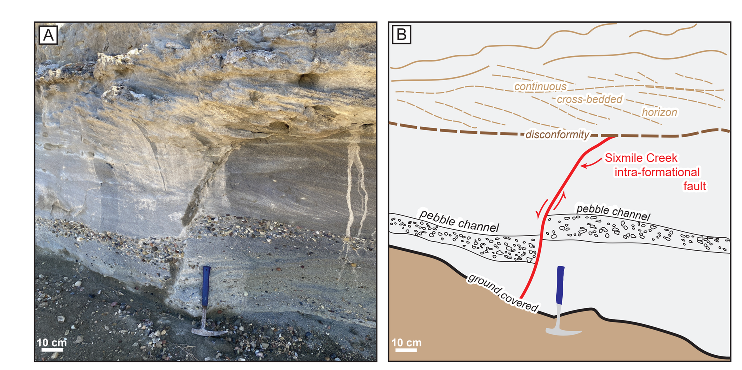

Figure 3. Field photograph (A) and interpretive sketch (B) Figure shows intraformational faulting within the Sixmile Creek Formation as indicated by the fluvial round pebble-filled channel offset in a normal sense. Note the continuous (not offset) overlying cross-bedded horizon at the top of the ~2-m outcrop.

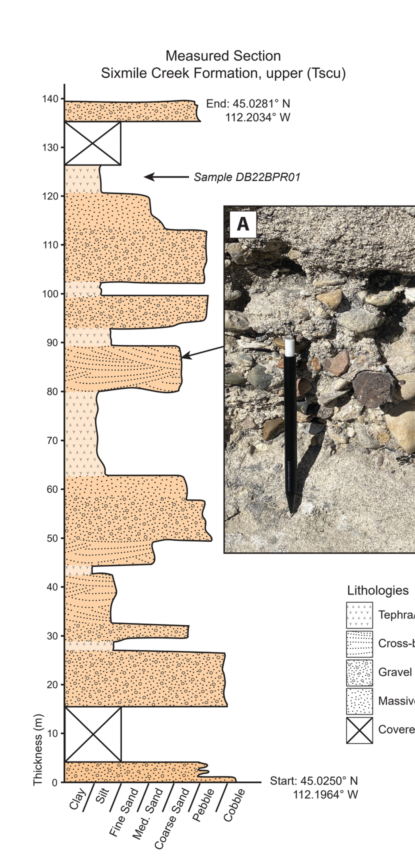

Figure 4. Measured stratigraphic section of conglomerate and tephra lithologies of the Big Hole River member and Anderson Ranch beds of the Sixmile Creek Formation. The stratigraphy shown above is representative of the lithologies that were mapped as Sixmile Creek Formation, undivided (Tscu). Inset photo A shows a likely Hemphillian-age limb fossil found within the measured section; pencil is approximately 15 cm (6 in).

REFERENCES

Constenius, K.N., 1996, Late Paleogene extensional collapse of the Cordilleran foreland fold and thrust belt: Geological Society of America Bulletin, v. 108, p. 20–39.
Fritz, W.J., and Sears, J.W., 1993, Tectonics of the Yellowstone hotspot wake in southwestern Montana: Geology, v. 21, p. 427–430.
Fritz, W.J., Sears, J.W., McDowell, R.J., and Wampler, J.M., 2007, Cenozoic volcanic rocks of southwestern Montana: Northwest Geology, v. 36, p. 91–110.
Garihan, J.M., 1979, Geology and structure of the central Ruby Range, Madison County, Montana: Geological Society of America Bulletin, v. 90, no. 4, pt. II, p. 695–788, https://doi.org/10.1130/GSAB-P2-90-695
Garson, Y.N., 1992, Cenozoic volcanism and extensional tectonics of the Timber Hill map area, southwestern Montana: disruption of a Neogene paleovalley: Missoula, University of Montana, M.S. thesis, 51 p.
Harms, T.A., and Baldwin, J.A., 2020, Paleoproterozoic geology of Montana, *in* Metesh, J.J., and Vuke, S., eds.: Montana Bureau of Mines and Geology Special Publication 122: Geology of Montana—Geologic History, v. 1, 65 p., available at https://mbmg.mtech.edu/pdf/geologyvolume/HarmsBaldwin_PaleoproterozoicFinal.pdf
Heinrich, E.W., 1960, Geology of the Ruby Mountains and nearby areas in southwestern Montana, *in* Pre-Beltian geology of the Cherry Creek and Ruby Mountains areas, southwestern Montana: Montana Bureau of Mines and Geology Memoir, v. 38, p. 31–62.
James, H.L., 1990, Precambrian geology and bedded iron deposits of the southwestern Ruby Range, Montana: U.S. Geological Survey Professional Paper, v. 1495, p. 1–39.
Kuenzi, W.D., and Fields, R.W., 1971, Tertiary stratigraphy, structure, and geologic history, Jefferson Basin, Montana: Geological Society of America Bulletin, v. 82, p. 3373–3394.
Mogk, D.W., Mueller, P.A., and Henry, D.J., 2020, The Archean geology of Montana, *in* Metesh, J.J. and Vuke, S., eds.: Montana Bureau of Mines and Geology Special Publication 122: Geology of Montana—Geologic History, v. 1, 45 p., available at https://mbmg.mtech.edu/pdf/geologyvolume/Mogk_ArcheanFinal.pdf
Monroe, J.S., 1976, Vertebrate paleontology, stratigraphy, and sedimentation of the upper Ruby River basin, Madison County, Montana: Missoula, University of Montana, Ph.D. dissertation, 301 p.
Mosolf, J.G., and Sears, J.W., 2024, Geologic map of the Red Canyon 7.5′ quadrangle, Beaverhead and Madison counties, Montana: Montana Bureau of Mines and Geology Geologic Map 95, 1 sheet, scale 1:24,000.
Mosolf, J.G., 2021, Geologic map of the Virginia City 7.5′ quadrangle, Madison County, Montana: Montana Bureau of Mines and Geology Geologic Map 80, 1 sheet, scale 1:24,000.
Mosolf, J.G., Brennan, D.T., Gavillot, Y., Parker, S., and Sears, J., 2023a, Major oxide and trace element analyses of rock samples collected in the Dillon and Hamilton 30' x 60' quadrangles, southwest Montana: Montana Bureau of Mines and Geology Analytical Dataset 2.
Mosolf, J.G., Brennan, D.T., and Kylander-Clark, A., 2023b, LA-ICPMS U-Pb geochronology data from rock samples collected in the Dillon, Ennis, Gardiner, Hamilton, Hebgen Lake, and Wisdom 30' x 60' quadrangles, western Montana, 2022–2023: Montana Bureau of Mines and Geology Analytical Dataset 5.
Petkewich, R.M., 1972, Tertiary geology and paleontology of the Beaverhead East area, southwestern Montana: Missoula, University of Montana, Ph.D. dissertation, 365 p.
Ripley, A., 1987, Paleoenvironmental interpretation of Tertiary carbonates in western Montana: Missoula, University of Montana, M.S. thesis, 99 p.
Ruppel, E.T., O'Neill, J.M., and Lopez, D.A., 1993, Geologic map of the Dillon 1º x 2º quadrangle, Idaho and Montana: U.S. Geological Survey Miscellaneous Investigations Series Map I-1803-H, scale 1:250,000.
Stotter, S.V., 2019, Determining the Precambrian structure and thermotectonic evolution of the central Ruby Range, southwest Montana: Missoula, University of Montana, M.S. thesis, 78 p.
Thomas, R.C., and Sears, J.W., 2020, Middle Miocene through Pliocene sedimentation and tectonics in Montana: A record of the outbreak and passage of the Yellowstone Hotspot, *in* Metesh, J.J., and Vuke, S., eds.: Montana Bureau of Mines and Geology Special Publication 122: Geology of Montana—Geologic History, v. 1, 25 p., available at https://mbmg.mtech.edu/pdf/geologyvolume/ThomasAndSears_SixmileCreekFinal.pdf
Vuke, S.M., 2020, The Eocene through early Miocene sedimentary record in western Montana, *in* Metesh, J.J., and Vuke, S., eds.: Montana Bureau of Mines and Geology Special Publication 122: Geology of Montana—Geologic History, v. 1, 38 p. https://mbmg.mtech.edu/pdf/geologyvolume/VukeLowerBozemanFinal.pdf
Woods, A.J., Omernik, J.M., Nesser, J.A., Shelden, J., Comstock, J.A., and Azevedo, S.H., 2002, Ecoregions of Montana, 2nd ed. (color poster with map, descriptive text, summary tables, and photographs): Reston, Va., U.S. Geological Survey, scale 1:1,500,000.

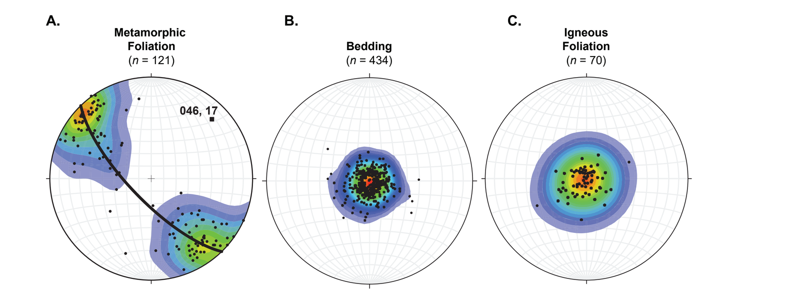

Figure 5. Lower-hemisphere projection stereogram of poles to plane measurements for all measured (A) metamorphic foliations, (B) bedding surfaces and, (C) igneous foliations. The data are plotted on an equal-area stereonet and fit with Kamb contours. In stereogram (A) the great circle represents the cylindrical best fit of the metamorphic foliations with the corresponding trend and plunge of the fold hinge marked by the labeled black square.

TABLE 1. Major oxide and trace element geochemistry.

Sample ID	JM22BPR03	DB22BPR04	DB22BPR05
Map unit	Tsr	Adg	Adg
Lithology	Rhyolite	Amphibolite	Gneiss
Latitude (°N)	45.0778	45.0954	45.0944
Longitude (°W)	112.2178	112.2462	112.2450
Major Elements (wt %)			
SiO_2	81.93	50.22	76.03
TiO_2	0.44	0.79	0.32
Al_2O_3	10.27	15.32	11.13
FeO*	0.87	10.65	3.62
MnO	0.00	0.18	0.03
MgO	0.27	8.21	0.13
CaO	0.21	10.93	1.12
Na_2O	0.11	1.98	2.80
K_2O	1.62	0.49	3.83
P_2O_5	0.09	0.07	0.07
Sum	95.82	98.85	99.07
LOI	3.87	0.81	0.49
Trace Elements (ppm)			
Ni+	10.9	158.9	2.7
Cr+	74.5	502.8	8.9
V+	67.8	333.9	11.8
Ga+	18.5	19.4	25.6
Cu+	11.7	139.0	1.6
Zn+	25.7	110.2	99.8
La	30.5	3.6	60.0
Ce	56.6	8.4	124.6
Pr	6.5	1.3	12.8
Nd	23.9	6.1	45.7
Sm	4.4	2.0	8.6
Eu	0.9	0.7	1.6
Gd	3.6	2.5	7.3
Tb	0.5	0.5	1.2
Dy	3.2	3.0	7.2
Ho	0.7	0.7	1.5
Er	1.9	1.9	4.3
Tm	0.3	0.3	0.7
Yb	1.8	1.9	4.2
Lu	0.3	0.3	0.7
Ba	328.6	117.6	1,482.5
Th	9.7	0.5	24.6
Nb	14.4	2.1	15.1
Y	19.0	17.9	38.6
Hf	5.3	1.3	13.1
Ta	1.1	0.3	1.0
U	2.1	0.2	2.6
Pb	11.8	15.9	36.3
Rb	61.7	10.1	104.0
Cs	7.2	0.1	0.4
Sr	110.1	119.6	70.4
Sc	6.0	36.5	2.9
Zr	190.5	45.1	485.5

Major elements and trace elements denoted by + were analyzed by XRF; all other trace elements were measured by ICP-MS. FeO* indicates all Fe expressed as Fe^{2+}.
All samples analyzed by X-ray fluorescence (XRF) and inductively coupled plasma mass spectrometry (ICP-MS) at the Washington State University GeoAnalytical Lab.
Datum used for sample coordinates is World Geodetic Survey 1984 (WGS84).
Complete geochemical data available from Mosolf and others (2023a).

Table 2. U-Pb zircon geochronology

Sample	Lithology	Unit	Latitude (°N)	Longitude (°W)	Method	No. of Spot Analyses[a]	Age (Ma)	2σ	MSWD
JM22BPR01	vitric tuff	Tscu	45.0330	-112.2415	WM 206/238	33/49	8.2	0.1	2.6
DB22BPR01	tephra	Tscu	45.0281	-112.2033	WM 206/238	25/40	8.9	0.1	2.3
DB22BPR03	tephra	Tscu	45.0107	-112.1275	WM 206/238	35/40	10.1	0.1	2.6
SP22BPR01	tephra	Tscu	45.0761	-112.1975	MDA 206/238	21/46	14.1	0.2	0.8
DB22BPR02	tephra	Tscs	45.1225	-112.2202	WM 206/238	31/40	12.5	0.1	0.9
JM22BPR03	rhyolite	Tsr	45.0778	-112.2178	WM 206/238	12/90	34.0	0.7	3.1
JM22BPR02	welded tuff	Tsr	45.0679	-112.2342	WM 206/238	13/77	34.2	0.4	1.3
JM22BPR04	sandstone	Trpa	45.0532	-112.2421	See Fig. 2	-	-	-	-
DB22BPR05	gneiss	Adg	45.0944	-112.2450	MEA 207/206	16/72	2732	11	1.4

Note. Reported ages are the weighted mean of the ^{207}Pb corrected $^{206}Pb/^{238}U$ ages obtained for each sample. MSWD is the Mean Square Weighted Deviation.
Method: WM 206/238 weighted mean of select $^{206}Pb/^{238}U$ dates
MDA 206/238 max depositional age, weighted mean of youngest $^{206}Pb/^{238}U$ dates
MEA 207/206 maximum emplacement age, weighted mean of oldest overlapping $^{207}Pb/^{206}Pb$ dates
[a]Number of spot analyses used to calculate weighted mean age.
Zircon separates were prepared at the MBMG and analyzed by LA-ICPMS at the University of California, Santa Barbara, CA. Latitudes and longitudes are in the 1984 World Geodetic Survey (WGS84) datum.

Montana Bureau of Mines and Geology

Geologic Map 99

Geologic Map of the Belmont Park Ranch 7.5′ Quadrangle, Madison County, Montana

Daniel T. Brennan, James W. Sears, and Jesse G. Mosolf

2024
https://doi.org/10.59691/TJCH2055